RESEARCH ARTICLE

Spaceborne LiDAR for characterizing forest structure across scales in the European Alps

Lisa Mandl[1,2] (iD), Ana Stritih[1], Rupert Seidl[1,2], Christian Ginzler[3] & Cornelius Senf[1]

[1]Ecosystem Dynamics and Forest Management Group, School of Life Sciences, Technical University of Munich, Munich, Germany
[2]Berchtesgaden National Park, Berchtesgaden, Germany
[3]Swiss Federal Institute for Forest, Snow and Landscape Research WSL, Zurich, Switzerland

Abstract

The launch of NASA's Global Ecosystem Dynamics Investigation (GEDI) mission in 2018 opens new opportunities to quantitatively describe forest ecosystems across large scales. While GEDI's height-related metrics have already been extensively evaluated, the utility of GEDI for assessing the full spectrum of structural variability—particularly in topographically complex terrain—remains incompletely understood. Here, we quantified GEDI's potential to estimate forest structure in mountain landscapes at the plot and landscape level, with a focus on variables of high relevance in ecological applications. We compared five GEDI metrics including relative height percentiles, plant area index, cover and understory cover to airborne laser scanning (ALS) data in two contrasting mountain landscapes in the European Alps. At the plot level, we investigated the impact of leaf phenology and topography on GEDI's accuracy. At the landscape-scale, we evaluated the ability of GEDIs sample-based approach to characterize complex mountain landscapes by comparing it to wall-to-wall ALS estimates and evaluated the capacity of GEDI to quantify important indicators of ecosystem functions and services (i.e., avalanche protection, habitat provision, carbon storage). Our results revealed only weak to moderate agreement between GEDI and ALS at the plot level (R^2 from 0.03 to 0.61), with GEDI uncertainties increasing with slope. At the landscape-level, however, the agreement between GEDI and ALS was generally high, with R^2 values ranging between 0.51 and 0.79. Both GEDI and ALS agreed in identifying areas of high avalanche protection, habitat provision, and carbon storage, highlighting the potential of GEDI for landscape-scale analyses in the context of ecosystem dynamics and management.

Introduction

Research on forest structure has a long tradition in forest ecology (Watt, 1947; Whittaker & Woodwell, 1969). Forest structure describes the number, size, and spatial arrangement of trees and other wooded elements, which is closely linked to ecosystem services (Andrew et al., 2014). Climate and land use change put increasing pressure on forest ecosystems globally, with profound impacts on forest structure (Bohn & Huth, 2017; McDowell et al., 2020). These impacts might be particularly pronounced in mountain forests because mountain areas warm 25–50% faster than the global average (Hock et al., 2019). Mountain forests provide essential functions and services to society, such as protection from natural hazards (e.g., rockfall, landslides, flooding, snow

avalanches) and provision of habitats to a wide variety of species (Sebald et al., 2019; Stritih et al., 2021). These functions and services are largely determined by forest structure, e.g., protective forests need a certain height and density to provide protection from avalanches (Baggio et al., 2022), and keystone species of mountains forests require a certain size and distribution of trees as their habitat, e.g., Kortmann et al. (2018). Characterizing forest structure hence enables tracking the response of mountain forests and the functions and services they provide to climate and land use change (Atkins et al., 2018; Felipe-Lucia et al., 2018).

Collecting field-based data on forest structure is labor-intensive and limited in extent, which has increased the interest in using remote sensing for complementing terrestrial approaches in providing information on forest structure. While optical remote sensing has provided large-scale insights into forest cover changes (Gao et al., 2020; Senf & Seidl, 2022; Winkler et al., 2021; Wulder et al., 2020;), optical data is limited in its capacity to estimate structural parameters (Tang et al., 2019). Active remote sensing techniques, such as Light Detection And Ranging (LiDAR), overcome many of these limitations and provide detailed information on forest structure (Jucker, 2022; Lefsky et al., 2002; Valbuena et al., 2020). LiDAR measures the three-dimensional structure of forests by emitting laser pulses and measuring the travel time of the emitting pulse. Due to the capability of LiDAR to penetrate tree canopies, its 3D point-clouds provide information not only about the horizontal structure of the top canopy, but also allow for describing the vertical structure of a forest canopy, including sub-canopy trees (Jarron et al., 2020). Most LiDAR data is acquired by aircrafts (i.e., airborne laser scanning [ALS]) and provides highly detailed wall-to-wall coverage at the level of forest landscapes. Yet, ALS is also characterized by high acquisition costs, often irregular acquisition times and limited spatial coverage (Hancock et al., 2019), limiting the assessment of forest structure across large spatial extents as well as its application in regular monitoring efforts.

Spaceborne LiDAR systems can overcome some of the limitations described for ALS above, with various missions being available for different purposes: measuring the polar ice sheet mass balance (ICESat, ICESat-2) (Schutz et al., 2005), aerosols and clouds (CALIPSO) (Winker, 2007) as well as wind speed (Aeolus) (Banyard et al., 2021). None of these missions primarily targeted vegetation structure and their applicability to forests is thus limited (Dubayah et al., 2020). This gap was filled with the launch of NASA's Global Ecosystem Dynamics Investigation (GEDI) system. GEDI is a spaceborne LiDAR sensor that is specifically designed for characterizing forest ecosystems (Dubayah et al., 2020). GEDI is mounted on the International Space Station and started its data acquisition in April 2019, covering all terrestrial areas globally between 51.6° N/S in a sample-based approach. Since the early 2020, GEDI's scientific products are available via NASA's Land Processes Distributed Active Archive Center, including a set of ready-to-use structural metrics such as plant area index (PAI), foliage height diversity (FHD) or canopy cover (Dubayah et al., 2020; Fayad, Ienco, Baghdadi, et al., 2021).

Even though GEDI considerably advances our ability to quantify vegetation structure across large extents, important caveats need to be considered, particularly when applying GEDI in complex mountain areas. First, LiDAR metrices are sensitive to seasonal changes in foliage (Li et al., 2018). As the leaf-on period is short in many mountain regions, phenological effects are likely to influence GEDI metrics in mountain forests. Second, previous studies have shown that the accuracy of GEDI depends on sampling density (Schneider et al., 2020). Inherent to GEDI's sampling design, sampling densities are low in highly-fragmented landscapes, such as mountain areas, resulting in reduced accuracy. Third, it can be challenging to separate ground and vegetation returns in steep terrain (Fayad, Baghdadi, Alvares, et al., 2021). Compared to other spaceborne LiDAR instruments, GEDI has a smaller footprint of 25 m, which was designed to minimize such slope effects (Duncanson et al., 2022). However, the footprint is still relatively large compared to ALS data (~0.25 m), and a substantial bias can be expected when using GEDI to estimating forest height on steep slopes (Fayad, Baghdadi, Alcarde Alvares, et al., 2021; Ni et al., 2021). The degree to which these factors are limiting the use of GEDI for ecological applications in mountain areas remains unclear to date. However, a tool such as GEDI might be particularly valuable in mountains, where accessibility for field-based assessments is often low and where strong environmental gradients make large-scale assessments particularly insightful.

Here, our objective was to assess the applicability of GEDI data for characterizing the structure of mountain forests. To address this objective, we first analyzed how well GEDI performs in comparison to ALS in estimating key forest structural parameters at the plot scale. Specifically, we quantified the trade-off between GEDI data acquired through a longer period of time during the year (resulting in higher data density) and a potential seasonal/phenological mismatch to the reference ALS data. Furthermore, we evaluated the impact of topography on the estimation of structural parameters. Second, we investigated whether the sampling-based approach of GEDI is able to capture the variability in forest structure at the landscape scale, specifically analyzing whether rare cases are under-sampled by GEDI. We subsequently assessed how well GEDI is able to inform indicators of ecosystem

functions and services, focusing particularly on protection against avalanches, carbon storage, and habitat quality. We conducted our study in two contrasting mountain landscapes in Germany and Switzerland (Berchtesgaden and Davos), to study our questions under a range of different ecological conditions (inner mountains vs. front range, calcareous *vs.* crystalline geology etc.).

Materials and Methods

Study sites

We selected two study sites (Fig. 1) in the European Alps that represent a wide gradient of biophysical features and forest types. Berchtesgaden is situated in the southeastern part of Germany in the northern limestone Alps. We focused our analyses on Berchtesgaden National Park, an IUCN category 2 protected area of 20 808 ha. In total,

54% (11 835 ha) of the landscape is covered by forests, of which 54% are evergreen coniferous forests, 32% are mixed forests, 12% are larch-dominated forests and 2% are broadleaved forests (Lotz, 2006). Dominant tree species are Norway spruce [*Picea abies* (L.) Karst.], European larch (*Larix decidua* L.) and European beech (*Fagus sylvatica* L.) (Becker, 2016; Thom & Seidl, 2022). The landscape is characterized by complex topography with steep slopes (average slope of 29°) and a high elevation gradient from 600 to 2700 m a.s.l., with the tree line at approximately 1700 m a.s.l. (Mayer, 1984). The forests were largely managed before the establishment of the National Park in 1978, and legacies of past land use are still shaping current vegetation structure and composition.

The second study site, Davos, is located in the eastern part of Switzerland and is dominated by sub-alpine and alpine vegetation (1184–3181 m a.s.l.). The whole landscape is 45 216 ha in size, of which 16% (7200 ha) are
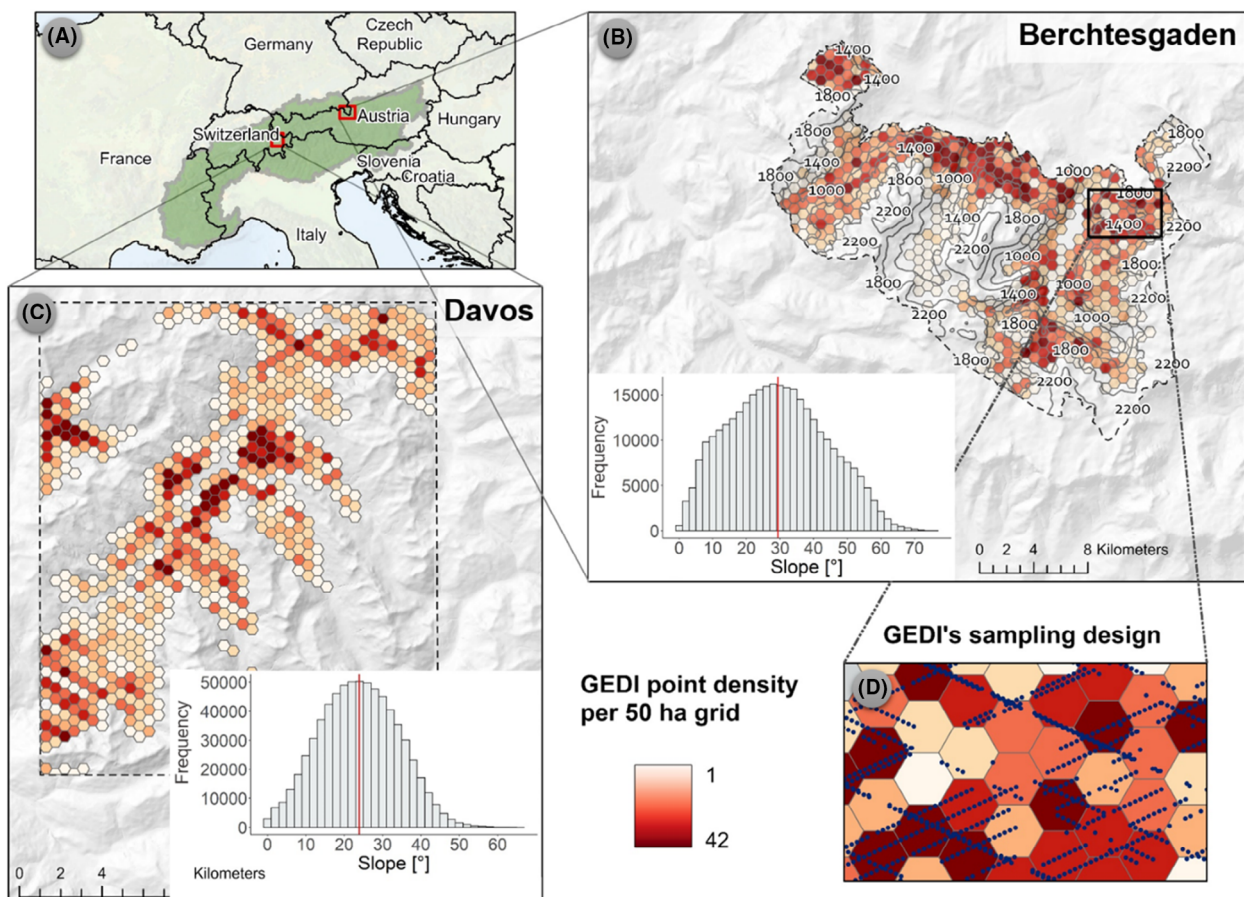
Figure 1. Overview map showing the location of the two study sites within the European Alps (dark green) (a). Hexagons in (b) and (c) show GEDI point density per 50 ha cell for the two study sites Berchtesgaden (b) and Davos (c). (d) Illustrates GEDI's sampling design, with GEDI footprints shown as blue points. The histograms in (b) and (c) show the distribution of slopes within both study sites. GEDI, Global Ecosystem Dynamics Investigation.

covered by forests. The forests are 84% evergreen coniferous, 13% larch-dominated and 3% mixed (AWN, 2019). In contrast to Berchtesgaden, Davos is more strongly dominated by conifers, in particular Norway spruce and European larch. The upper tree line in Davos occurs at approximately 2160 m a.s.l. (Mietkiewicz et al., 2017), and the average slope is 24°. Forests in Davos are largely managed, with the main management objective being the maintenance of the protective function of forests (AWN, 2018; Temperli et al., 2017).

Data

GEDI data

GEDI is a full-waveform laser-based instrument that samples footprints of 25 m diameter every 60 m along eight data tracks that are 600 m apart (Dubayah et al., 2020). For this study, we used GEDI level 2A (Dubayah, Hofton, et al., 2021) and 2B (Dubayah, Tang, et al., 2021) products. Due to higher geolocation accuracy, we only used version 2 data with a mean horizontal error of 10.3 m (Luthcke et al., 2019). Level 2A data contain elevation and percentiles of canopy height (Dubayah, Hofton, et al., 2020), while the level 2B data contain vegetation structural metrics such as PAI, FHD and canopy cover. The metrics are computed based on the directional gap probability from level 1B waveform data (Tang & Armston, 2019) using one out of six available algorithm settings. The algorithm setting groups mainly differ in their thresholds for detecting the background noise level and thus the way waveforms are interpreted (Hofton et al., 2019). Although the most appropriate algorithm is automatically selected for version 2 data, we calculated the metrics for all other non-default algorithm setting groups manually and checked their agreement with ALS data. Since this preliminary analysis showed that the default algorithm setting had the best correlation with reference data, we performed all further analyses with default settings.

We acquired 6766 and 4574 GEDI footprints for the Berchtesgaden and Davos study sites, respectively. We only used GEDI footprints that intersect with forests (using a forest type data sets described in more detail in section "Forest type data" below) and that met certain quality criteria expressed by quality flag = 1 and degrade flag = 0. Quality flags allow for filtering out low quality footprints based on energy, sensitivity, amplitude, real-time surface tracking quality, and differences to a digital elevation model (Beck et al., 2021). GEDI data acquisition and processing was conducted using the rGEDI package (v0.3.0) (Silva et al., 2020) in the R software environment for statistical computing and graphics (R Core Team, 2021).

Table 1. ALS acquisition parameters for Berchtesgaden and Davos.

Parameter	ALS Berchtesgaden	ALS Davos
Acquisition date	Sep. 2021	Aug.–Nov. 2020
Ø Point density (last pulses)	47.0 points/m^2	16.9 points/m^2
Wavelength	1064 nm	1064 nm
Horizontal accuracy	<40 cm	<20 cm
Vertical accuracy	<10 cm	<10 cm

ALS, airborne laser scanning.

ALS data

We used two ALS datasets available for both study sites (Table 1) to benchmark GEDI estimates. The main difference between the two LiDAR datasets was the time of data acquisition. While the ALS data in Berchtesgaden was recorded at the end of the leaf-on season in 2021, the ALS data from Davos was acquired at the beginning of the leaf-off season in 2020. Point densities also differed between both datasets (Table 1), but the horizontal and vertical accuracies were similar. Accuracy was checked by stripe overlap differences and deviations of the control points before and after the adjustment.

To derive metrics comparable to GEDI from ALS data, several pre-processing steps were applied. We performed an outlier removal on the ALS point clouds using a noise segmentation algorithm based on statistical outlier removal and applied a spatial interpolation using the Delaunay triangulation for point cloud normalization. All of the ALS processing was done using the lidR package (Roussel et al., 2020; Roussel & Auty, 2022) in R.

Forest type data

To test the effect of phenology on forest structure estimates from GEDI, we stratified our study sites into evergreen coniferous, deciduous coniferous, mixed, and broadleaved forests. For Berchtesgaden we used the HabitAlp dataset, a stereographic aerial interpretation of the dominant habitat type (Lotz, 2006), which we reclassified into the above mentioned classes. For Davos, we reclassified a forest stand map from 2019 (AWN, 2019) into the same classes.

Forest structural metrics

We computed a consistent set of forest structural metrics for both GEDI and ALS. Following the classification of Atkins et al. (2018), the metrics can be divided into groups describing *height, area and density, heterogeneity*

and *cover and openness*. For *height*, we used the relative heights (RHs) as percentiles of the vertical distribution at 50 and 98% of LiDAR first returns. The 50th percentile contains information about the distribution of tree size classes, e.g., important for forest planning (Næsset, 1997), whereas the 98th percentile corresponds to canopy top height. Specifically, RH(x) is the height above the ground below which x% of the backscattered energy is located in the waveform (Zolkos et al., 2013):

$$RHx = \Sigma \frac{x(n+1)}{100},$$

where x is the respective percentile and n is the total number of ordered z values within the plot.

Area and density were represented by the PAI for GEDI and the leaf area index (LAI) for ALS, which are important and widely used parameter in plant ecology (Fang et al., 2019; George et al., 2021) that are, e.g., indicative of the radiation absorbed by plant canopies. Although LAI quantifies only leaves, and not the total plant area such as PAI, the two indices are strongly related because leaf area is usually orders of magnitude larger than the tree's other components (Kucharik et al., 1998), i.e., LAI is a dominant component of PAI. We calculated LAI from ALS by first determining the leaf area density (LAD) profile of the canopy volume according to Bouvier et al. (2015), which is the total leaf area per unit volume:

$$LAD = -\Sigma \frac{\ln P(z)}{k},$$

where P is the gap fraction of the canopy to a given height z, and k is the extinction coefficient (here $k = 0.5$). Gap fraction P was computed following the approach proposed by Roussel et al. (2018):

$$P = \frac{N_{[0;z]}}{N_{[0;z+dz]}}$$

with $N_{[0;\ z]}$ being the number of returns below z and $N_{[0;\ z+dz]}$ the number of returns below $z + dz$ (dz describes the thickness of a forest layer in horizontal slices, here $dz = 1$ m). The LAD assesses the number of laser points actually reaching the predefined height bins (="thickness" of the layer) and those passing the layer (=gap fraction P). Subsequently, the log of this quantity is calculated and divided by extinction coefficient k as described in Bouvier et al. (2015). Finally, LAI is derived by integrating LAD $l(z)$ for all horizontal bins dz (here $dz = 1$ m):

$$LAI = \int_0^z l(z)dz.$$

To describe the *heterogeneity* of the canopy, we calculated FHD as defined by MacArthur and MacArthur (1961), a metric that is widely used to describe forest canopy complexity (Walter et al., 2021). FHD was computed based on the Shannon-Weaver information index (Shannon, 1948):

$$FHD = -\Sigma pi \ln pi,$$

where p_i is the proportion of horizontal vegetation in the ith layer (here: 1 m horizontal bins), corresponding to the ratio of LiDAR return in the ith layer to the total returns (Clawges et al., 2008; MacArthur & MacArthur, 1961). FHD quantifies the evenness and diversity of the point cloud's distribution across the canopy.

Cover and openness was described by total canopy cover and understory cover, the latter defined as vegetation cover below 5 m We used the 5 m threshold as it corresponds to the official forest definition of the FAO (2020), but other thresholds could have been chosen instead. Cover metrics describe the density of the canopy and are thus related to light availability on the floor and the growth of understory vegetation (Depauw et al., 2021). We determined cover through the ratio of the number of first returns (z_{first}) > 2 m to the total number of first returns (z_{first}):

$$\text{Canopy cover} = \Sigma \frac{z_{first} > 2}{z_{first}}.$$

As it is known that GEDI waveforms are affected by a potential mix of ground and vegetation returns (Fayad, Baghdadi, Alvares, et al., 2021), we used an adapted form of GEDI's cover metric. Based on the cumulative cover profile (in 5 m height bins) available in the GEDI level 2B, we computed the cover above 5 m to minimize the effect of mixing ground and vegetation returns (see also Schneider et al., 2020). We did not apply such a height threshold for the ALS derived cover metric. Understory cover was calculated in the same way, but the point cloud was previously filtered to include only points <5 m.

Statistical analysis

We modeled the relationship between ALS and GEDI-derived metrics by using standardized major axis regression (SMA) implemented in the smatr package (v3.4.8) (Warton et al., 2012). This statistical method assumes that there are errors in both X and Y variables, as opposed to ordinary least squares, which only assumes errors in the Y variable; (Warton et al., 2006). SMA regression is recommended when testing for the inter-dependence of two measurements, in our case airborne and spaceborne LiDAR (Warton & Weber, 2002). To estimate the parameters of the SMA, we used Huber's M estimation, which

is robust against outliers (Taskinen & Warton, 2011). We conducted this analysis for several subgroups (season, forest type, topographic pattern), which are explained in detail in the following.

Plot-scale analysis

First, we analyzed the plot-based agreement (plot here corresponding to the 25 m footprint size of GEDI) between the GEDI and ALS forest structure metrics as a function of time since ALS acquisition to assess the trade-off between GEDI data density (increasing with time since ALS acquisition) and seasonal mismatch (also increasing with time since ALS acquisition). The ALS data were collected at the end of the leaf-on season (mid-September) in Berchtesgaden and at the beginning of the leaf-off season (mainly in September and October) in Davos. We compared the GEDI and ALS data for acquisitions within ±3 weeks around ALS acquisition, within the full leaf-on and leaf-off season, as well as for the full year to investigate inter- and intra-seasonal effects. To maximize the number of footprints, we used data from all years GEDI was available (2020–2022), despite the ALS data being only available for 1 year. As temporal cutoff between leaf-on and leaf-off we selected mid-April and mid-September for both study sites. Based on these findings, we selected a final set of GEDI data to be used for subsequent analyses.

Subsequently, we examined whether seasonal effects on the relationship between GEDI and ALS are determined by forest phenology. To do this, we compared the agreement between GEDI and ALS metrics across various forest types: evergreen coniferous, deciduous coniferous, broadleaved and mixed. We subdivided coniferous forest stands into evergreen and deciduous to capture the effect of larch-dominated stands, which shed their needles in winter and hence are expected to show different seasonal effects. To further investigate the sensitivity of GEDI metrics to mountainous topography, we also compared the match between GEDI and ALS among different slope classes. Slope was computed from the ALS-based digital elevation model as the mean value within each 25 m GEDI footprint. We grouped slopes into flat (slope < 15°) gentle (15° ≤ slope < 35°) and steep (slope ≥ 35°) terrain.

Landscape-level analysis

At the landscape-level, we first assessed the performance of GEDI's sampling approach compared to wall-to-wall ALS metrics computing cumulative distribution plots. We gridded forest structure metrics at a 20 m resolution (400 m^2), which corresponds approximately the GEDI plot size (490 m^2). We evaluated whether GEDI is capable of capturing landscape-scale patterns of forest structure or whether biases are introduced by, e.g., under-sampling 'extreme' values. Besides this analysis, we gridded the mean values of GEDI and ALS metrics to a 50 ha hexagon grids and calculated agreement between both datasets at the landscape scale. We additionally tested 4 and 10 ha grids, but found that smaller grid sizes resulted in many empty grid cells with no GEDI footprint (over 50% of 4 ha cells and 30% of 10 ha cells were empty for both sites, whereas 20% of the 50 ha grid cells were empty). Finally, we derived a set of parameters indicative for important ecosystem functions and services from GEDI and compared them to the same indicators derived from ALS to explore GEDI's utility for questions of applied ecology. Avalanche protection is an important regulating service of mountain forests (Grêt-Regamey & Straub, 2006), which requires a sufficient canopy cover and tree height (Frehner et al., 2005). As proxy for habitat quality we used indicators of habitat suitability for capercaillie (*Teatro urogallus*), an umbrella species for avian biodiversity (Suter et al., 2002). Finally, we used height and PAI as proxies for forests' carbon storage (i.e. amount of aboveground biomass) and uptake capacity, respectively (Duncanson et al., 2022; Zhao et al., 2021). All indicators were evaluated on a binary scale for each grid cell: For avalanche protection and habitat quality, we defined thresholds above which these services and functions were positively evaluated (Table 2). Due to a lack of absolute thresholds and high spatial variability of carbon density (Seidl et al., 2012), we defined forests with a high carbon storage and uptake capacity as those in the top 25% of height and PAI (based on ALS data), which corresponds to RH98 > 24 m and PAI > 3.5 in our data and across both study sites.

Table 2. Assessed ecosystem functions and services and their criteria and thresholds.

Ecosystem functions and services	Criteria	Reference
Avalanche protection	Cover >50% AND height >5 m	Frehner et al. (2005)
Habitat suitability for capercaillie	FHD > 2 AND cover = [40; 70]	Graf et al. (2013); Suter et al. (2002)
High carbon uptake and storage	RH98 > 75th percentile AND PAI > 75th percentile	Site-adaptive thresholds

FHD, foliage height diversity; PAI, plant area index; RH, relative height.

Results

Plot-scale

The availability of high-quality GEDI data varied across phenological seasons, with a higher availability of leaf-on data in both study sites. In Berchtesgaden, 44% of the footprints (6766) passed the quality check, of which nearly 100% (6762) were recorded in the leaf-on season. For Davos, only 21% of the footprints (4574) passed the quality check and 77% of these (3519) were recorded in the leaf-on season. We observed a trade-off between the amount of GEDI footprints included in the analysis and the temporal proximity of GEDI data to the date of recording of the ALS data with regard to the agreement between GEDI and ALS (Table 3). The agreement between ALS and GEDI forest structural metrics was highest when the date of recording of both sensors corresponded closely. Agreement varied substantially between metrics, with R^2 values ranging from 0.0 to 0.52. Highest agreement was found for RH50/RH98 and FHD, but also for cover GEDI corresponded well to ALS (all $R^2 > 0.3$, see Table 3). Lower agreement was found for PAI and the relationship was weakest for understory cover. Including GEDI information for the whole leaf-on season increased data availability, but decreased agreement. An even stronger decrease in agreement was observed for only using leaf-off observations, especially for metrics depending on leaf area (i.e., PAI, cover and FHD). Using data for the full phenological season (i.e., leaf-on and leaf-off) improved agreement compared to using leaf-on data for Berchtesgaden but not for Davos. Based on these analyses, we chose two different time windows for both study sites for subsequent analyses. For Berchtesgaden, we used data in close temporal proximity (± 3 weeks) to the ALS acquisition ($n = 2806$). For Davos, however, data from the leaf-on season was used ($n = 3519$) because there were too few observations in close proximity to the ALS date for further stratification of the data.

The agreement between GEDI and ALS also differed by forest type, but these differences were not consistent across both study areas. In Berchtesgaden, the agreement was highest in broadleaved deciduous stands for most metrics (Table 3), while RH98, FHD and cover were also captured well in evergreen coniferous forests. In Davos, where no broadleaved forests were present, evergreen coniferous forests had the highest agreement for most metrics, but FHD performed better in deciduous coniferous forests.

Finally, the degree of agreement between GEDI and ALS was generally highest in flat terrain ($<15°$) and decreased with increasing angle of slope and was especially low on steep slopes $>35°$. Moving from moderately

Table 3. Agreement between GEDI and ALS (R^2 values) by different seasons, forest types, and slope classes.

	Season				Forest type				Slope		
	ALS	Leaf-on	Leaf-off	Full	Broadleaved	Evergreen conif.	Deciduous conif.	Mixed stands	<15°	<35°	>35°
# GEDI footprints	2806	6762	4	6766	338	1163	262	1043	302	1491	1010
RH50	0.33	0.22	0.14	0.26	0.38	0.31	0.07	0.33	0.61	0.57	0.16
RH98	0.36	0.26	0.20	0.29	0.36	0.38	0.30	0.30	0.50	0.55	0.29
PAI	0.23	0.16	0.11	0.18	0.31	0.22	0.03	0.22	0.44	0.34	0.11
FHD	0.38	0.23	0.07	0.26	0.28	0.41	0.30	0.23	0.37	0.41	0.26
cover	0.33	0.25	0.09	0.29	0.37	0.36	0.16	0.35	0.58	0.46	0.20
Understory cover	0.00	0.00	0.09	0.00	0.00	0.00	0.00	0.02	0.06	0.00	0.00
# GEDI footprints	512	3519	1055	4574	0	2971	499	49	322	2218	979
RH50	0.32	0.24	0.17	0.23	-	0.22	0.07	0.02	0.28	0.29	0.18
RH98	0.52	0.35	0.31	0.35	-	0.32	0.21	0.32	0.45	0.38	0.28
PAI	0.18	0.12	0.09	0.12	-	0.10	0.10	0.04	0.18	0.15	0.11
FHD	0.38	0.25	0.19	0.25	-	0.18	0.20	0.01	0.33	0.29	0.22
cover	0.31	0.21	0.16	0.21	-	0.17	0.13	0.01	0.31	0.24	0.18
Understory cover	0.02	0.00	0.00	0.00	-	0.00	0.02	0.03	0.06	0.00	0.00

(Berchtesgaden = upper block; Davos = lower block)

The season "ALS" indicates the time period ± 3 weeks around the time of the ALS flight. Green colors indicate high R^2, yellow marks intermediate ranges while ocher indicates low R^2. ALS, airborne laser scanning; FHD, foliage height diversity; GEDI, Global Ecosystem Dynamics Investigation; PAI, plant area index; RH, relative height.

slopes to steep slopes, agreement decreased more strongly than between flat terrain and moderate slopes, indicating that slope effects were non-linear across slope angles. However, flat areas also had the largest biases for cover-related metrics, with PAI and cover being systematically underestimated by GEDI in flat terrain (Fig. 2). This bias was particularly large at forest edges and in open forests. Height-related metrics were overestimated on steeper slopes, while FHD was least sensitive to slope at both study sites.

Landscape-level

In a comparison of the distributions derived from GEDI data to wall-to-wall ALS metrics, we found general agreement between patterns across metrics and study sites. Height metrics were overestimated by GEDI, while cover metrics were underestimated (Fig. 3). We checked whether underestimation was related to our adjusted cover calculation, but using the default cover metric led to even weaker agreement at the plot level, and still underestimated ALS-derived cover at the landscape level. For FHD, we found an inflection point, indicating that GEDI overestimates vertically simple structures and underestimates more complex stands. Consistent with the plot level comparison, the results for understory cover were poor.

The gridded GEDI metrics represented the spatial patterns of forest structure well, resulting in higher R^2 values at the landscape scale compared to plot-level analyses (Table 4; Fig. 4). We observed high agreement for height and vertical structure metrics and only slightly lower agreement for total canopy cover. For understory cover, however, GEDI's performance remained weak. The observed spatial patterns were similar for both GEDI and ALS, but GEDI tended to overestimate spatial variability on the landscape (Fig. 4). Analyzing the distribution of differences (Fig. 4) we found similar patterns across sites, with a slight to medium overestimation of height metrics and underestimation of cover metrics. For PAI and FHD, both over- and underestimation occur with similar frequencies.

Deriving indicators of important ecosystem functions and services (Table 5; Fig. 5) from metrics of forest structure, we found high agreement between GEDI and ALS for avalanche protection and habitat suitability. GEDI predicted the same percentage of forests fulfilling the criteria of each indicator as ALS. We also found high spatial
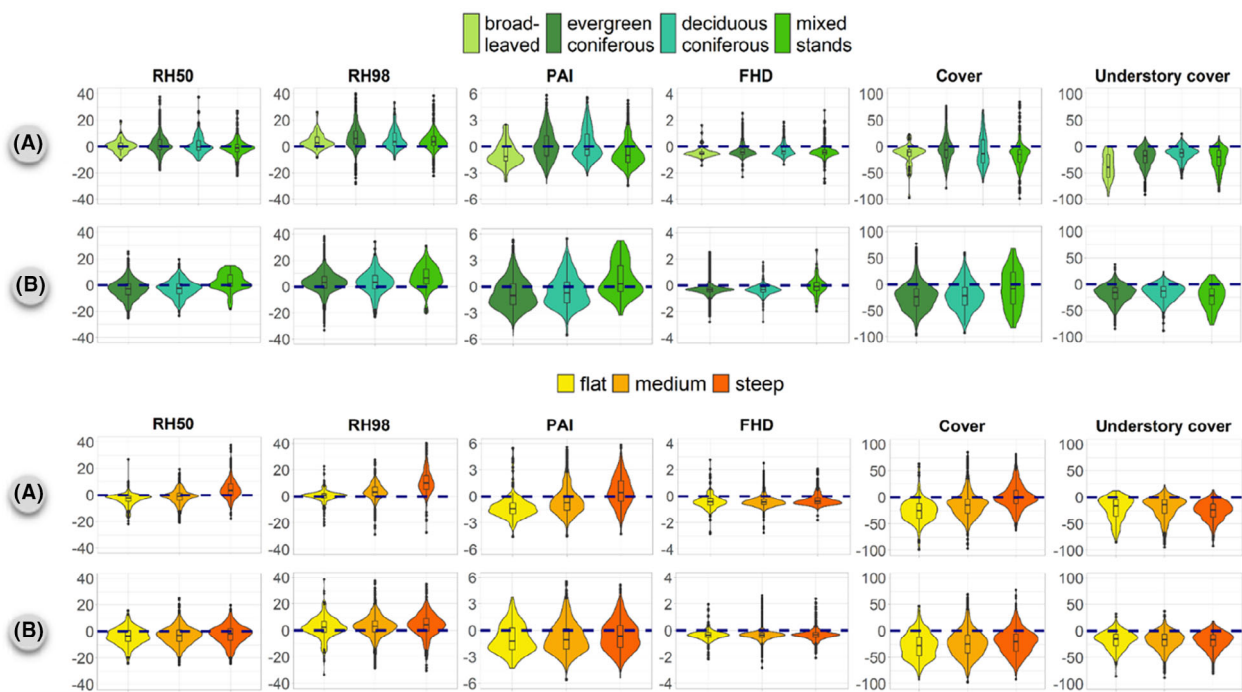

Figure 2. Differences between plot-level GEDI and ALS data grouped by forest type and slope category (flat = <15°, 15° < moderate = ≤35°, steep = >35°). The first row of each group represents the Berchtesgaden study site (a) and the second row Davos (b). Violin plots show the empirical density distribution of the data, boxplots within the violins indicate the median values (horizontal line), interquartile range (limited by 25th and 75th quantile) and outliers (>1.5 interquartile range below/above the 25th and 75th quantile). ALS, airborne laser scanning; GEDI, Global Ecosystem Dynamics Investigation.
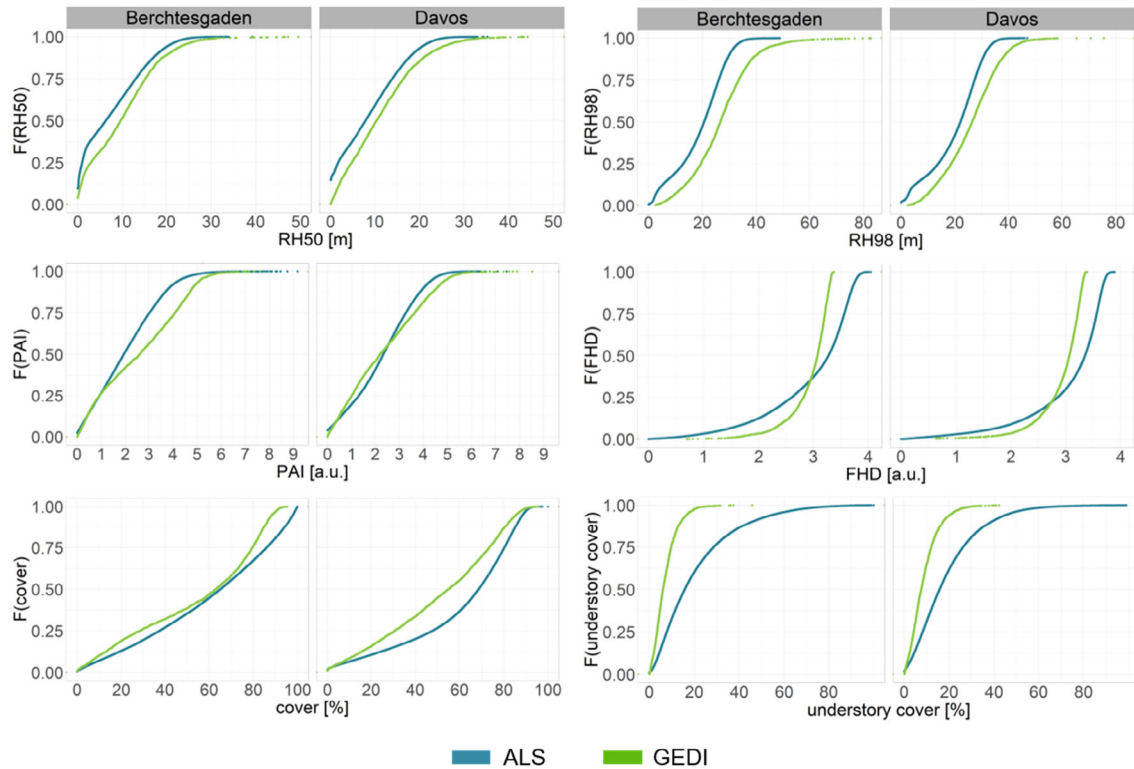
Figure 3. Cumulative density distributions, comparing wall-to-wall (ALS) and sample-based (GEDI) metrics of forest structure at the landscape level. If the GEDI line is above the ALS line, there is an underestimation of the metrics by GEDI. Conversely, GEDI below ALS indicates overestimation. ALS, airborne laser scanning; GEDI, Global Ecosystem Dynamics Investigation.

Table 4. Landscape-scale agreement (R^2) between ALS and GEDI metrics, aggregated at 50-ha hexagon grids.

	RH50	RH98	PAI	FHD	Cover	Understory cover
Berchtesgaden	0.67	0.73	0.68	0.71	0.54	0.03
Davos	0.66	0.79	0.63	0.71	0.51	0.01

ALS, airborne laser scanning; FHD, foliage height diversity; GEDI, Global Ecosystem Dynamics Investigation; PAI, plant area index; RH, relative height.

agreement between ALS and GEDI-derived metrics for both indicators. For carbon uptake and storage, our results revealed somewhat larger discrepancies between GEDI and ALS. Consistently across both sites, GEDI estimated a higher proportion of the landscape to have high carbon uptake and storage compared to ALS.

Discussion

Here we show that GEDI-based forest structural metrics match ALS-based metrics with only moderate accuracy at the plot level, but that agreement is high for landscape-level metrics and indicators of ecosystem functions and services. Despite limitations in making plot-level predictions, GEDI is thus a useful tool for ecological analysis at the landscape scale. Its utility is further amplified by the free availability and near-global coverage of GEDI (i.e., <51.6° N and >51.6° S). Further, GEDI provides a set of "ready-to-use" metrics that do not require any additional computation or in-depth knowledge of LiDAR technology. This makes GEDI interesting for ecologists not trained in remote sensing analysis. That said, we describe several factors limiting the applicability of GEDI data, especially in complex terrain such as the mountainous landscapes investigated here. Keeping those limitations in mind is important for ecologists applying GEDI data to their study system.

GEDI is designed as a sample-based instrument and thus provides data only for a subset of the Earth's surface. We identified a trade-off between sample size and time window of interest (which could be a summer maximum, a certain disturbance event, etc.) that needs to be considered when using GEDI data. Phenology was particularly important for metrics describing the distribution of vegetation in the canopy, as foliage determines how laser beams are backscattered. Depending on the goal of the
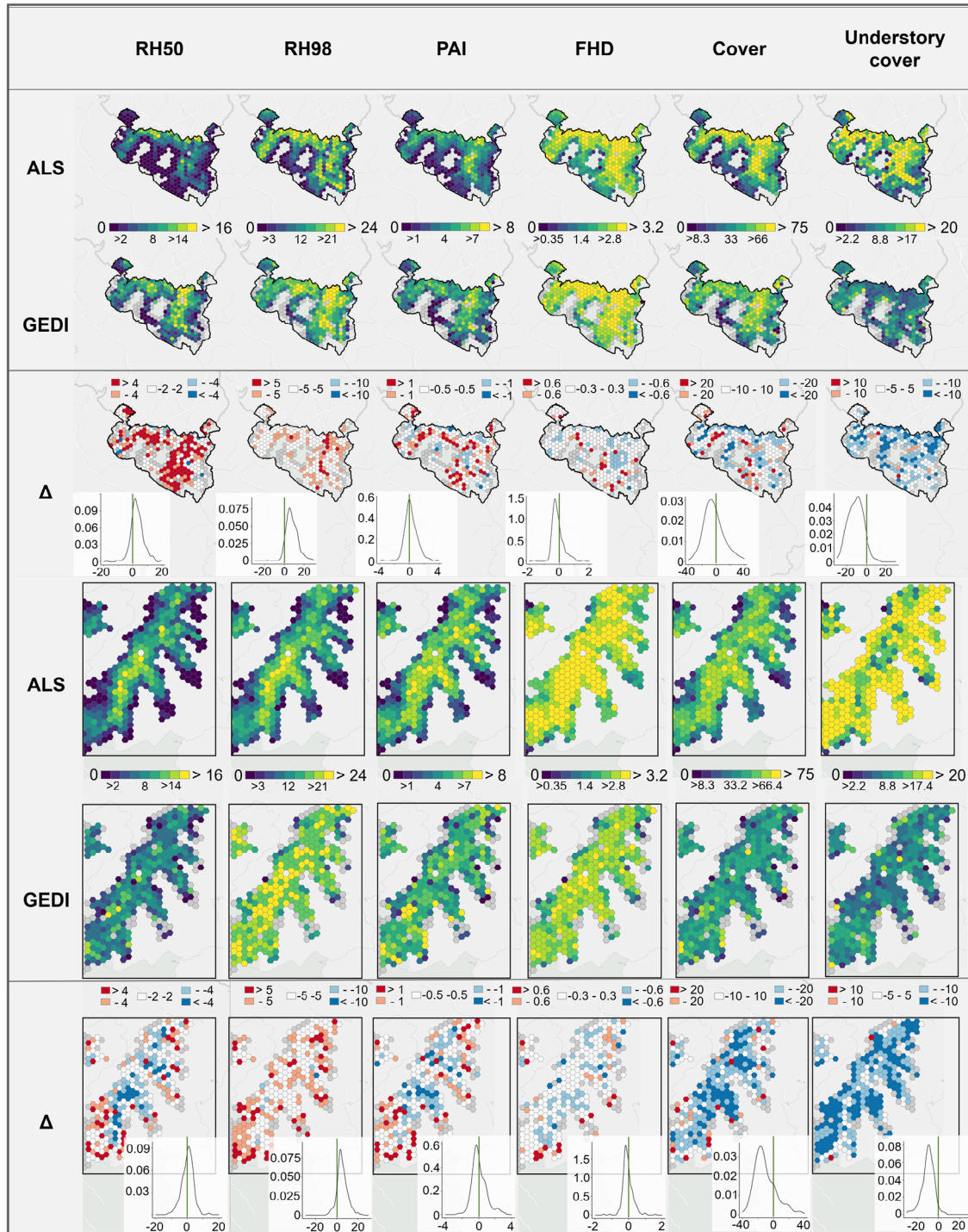
Figure 4. Landscape-scale analysis of ALS- and GEDI metrics gridded to 50 ha hexagons. The first three rows represent the Berchtesgaden study site, the last three rows Davos. Δ represents difference grids resulting from GEDI–ALS. Density plots show the distribution of the deviance around 0 (=ALS value) and indicate over- and underestimation. Top three lines: Berchtesgaden; bottom three lines: Davos. ALS, airborne laser scanning; GEDI, Global Ecosystem Dynamics Investigation.

Table 5. Percentage of the forested landscape fulfilling the criteria for selected ecosystem functions and services, derived from GEDI and ALS metrics of forest structure.

Ecosystem service indicator	Berchtesgaden		Davos	
	GEDI	ALS	GEDI	ALS
Avalanche protection	51%	48%	37%	36%
Habitat suitability for capercaillie	41%	41%	58%	58%
High carbon uptake and storage	30%	17%	25%	15%

ALS, airborne laser scanning; GEDI, Global Ecosystem Dynamics Investigation.

analysis, caution should be taken in selecting only observations from the leaf-on season, which becomes especially important in mountain landscapes with short growing seasons. We found generally lower agreement between GEDI and ALS in deciduous coniferous stands, likely due to larches having a more open canopy and weaker backscatter compared to other deciduous trees (e.g., beech), which form denser canopies and thus have stronger backscatter (Heurich & Thoma, 2008). In addition, the conical shape of conifers affects the height-related metrics as the probability of a laser pulse intercepting the apex of the crown is low (Lim et al., 2003; Næsset, 1997). Depending on the local species community and forest type, a variable performance of GEDI can thus be expected; this should be taken into consideration before applying GEDI data. We also found that estimates of understory cover cannot be reproduced reliably by GEDI. Especially for forests with dense canopy cover, the return backscattered from the forest floor is rather weak, making it difficult to detect this signal against high background noise (Dubayah et al., 2020). Further, disentangling ground and understory vegetation returns is challenging as both signals are mixed in the waveform. This is the reason for the underestimation of FHD by GEDI (Schneider et al., 2020), a bias which we also observed for higher FHD values (>2.5) in our analysis.

In agreement with other studies, we identified topography as one of the strongest drivers of uncertainty in GEDI-based forest structural metrics. The negative relationship between slope and GEDI performance has been explained by the fact that laser waveforms can be strongly elongated in steep terrain (Schneider et al., 2020). The overestimation of height-related metrics in our analysis can thus be, at least partly, attributed to the slope bias (see also Adam et al., 2020; Kutchartt et al., 2022; Lang et al., 2022; Liu et al., 2021) GEDI's canopy height estimates are further strongly affected by vegetation height and canopy cover. As shown by Kutchartt et al. (2022), GEDI tends to overestimate canopy height for low vegetation and low canopy cover. Having an alpine study site characterized by a large height gradient and partially highly fragmented forest cover, these two aspects may be considered as additional drivers of GEDI's overestimation of height. Another reason is that GEDI is not able to distinguish vegetation from other objects like rocks, leading to the incorporation of such objects in the measurements (Potapov et al., 2021). Slope correction algorithms are available for addressing the slope bias of GEDI (e.g., Wang et al., 2019). However, implementing these algorithms is not straightforward and usually requires auxiliary data (e.g., high-quality digital elevation models; Fayad, Baghdadi, Alcarde Alvares, et al., 2021; Hancock et al., 2019; Ni et al., 2021). This limits the use of GEDI in data-poor regions and as a
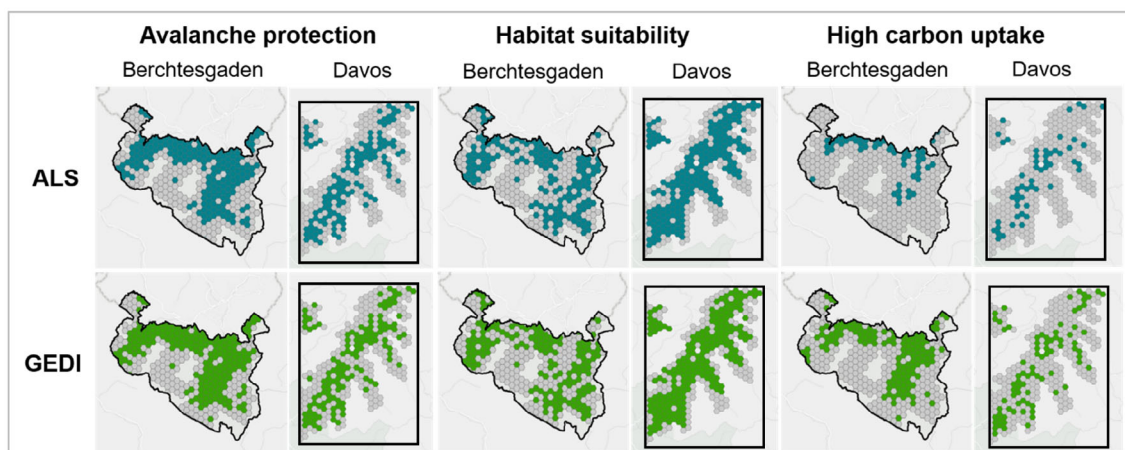

Figure 5. ALS and GEDI grid cells that fulfill the criteria for the provisioning of the ecosystem functions and services "avalanche protection", "habitat suitability" and "high carbon uptake". Grey grid cells indicate that the criteria were not fulfilled. ALS, airborne laser scanning; GEDI, Global Ecosystem Dynamics Investigation.

'ready-to-use' product for ecologists. Novel data-driven algorithms (e.g., Lang et al., 2022 present a promising new way to address the issue of topographic, but are not yet operational). In addition to slope effects, a recent study found that the expected geolocation error of 10 m may account for more than 50% of the uncertainty in GEDI-derived height metrics (Roy et al., 2021). Assuming that this also applies for structural metrics, geolocation can be considered a further factor introducing uncertainty in mapping forest structure with GEDI.

Besides these GEDI-related limitations, the different point density of the ALS reference data from Berchtesgaden and Davos might be an additional source of uncertainty. However, we assume that the effect of the different point densities is only minor. As shown in Garcia et al. (2017), different point densities of ALS data mainly affect the metrics derived from a canopy height model, but not the metrics derived directly from the point clouds, as done in this study. Further, Garcia et al. (2017) and LaRue et al. (2022) found metrics-specific point density thresholds, which vary between 1 and 7.5 points/m^2. Even though the ALS data from the study site in Davos feature lower point density, it is still distinctively higher than the critical threshold defined in these studies.

Finally, GEDI is intended for global applications (Dubayah et al., 2020). In this study, we tested the application of this global product locally, specifically for two relatively small study sites in the European Alps. In doing so, we faced an "agreement gradient" from the plot- to the landscape scale and finally to indicators of relevance for ecological applications, with increasing agreement between GEDI and ALS with increasing scale and level of abstraction. Especially when considering indicators of relevance for applied ecological questions, GEDI showed promising potential for characterizing mountain forest ecosystems. This might be especially true for ecological indicators that are strongly related to forest structure, such as avalanche protection. GEDI is thus a valuable instrument for deriving landscape-level estimates of forest functions and services, despite only moderate performance at the plot scale. This makes GEDI a rich data source for ecological studies in adjacent fields, such as ecological modelling (Blaschke et al., 2004; Hiltner et al., 2022; Thom et al., 2022), assessment of ecosystem services (Coops et al., 2016; Melin et al., 2018; Moeslund et al., 2019; Vauhkonen, 2018) and the evaluation of post-disturbance forest development (Gelabert et al., 2020; Viana-Soto et al., 2022).

Conclusion

We compared metrics of forest structure derived from GEDI to ALS-based metrics in two mountain landscapes of the Alps. Our results support previous findings of a topographic bias in GEDI's canopy height estimates, and highlights that this bias also applies to other structural metrics provided by GEDI. We further show that phenology and forest types affect the estimation of forest structure from GEDI. Nonetheless, when analyzed at the landscape level the agreement between GEDI and ALS was satisfactorily, suggesting that GEDI is a promising tool for landscape-scale analysis of mountain forest structure. We further show that indicators describing the ability of forests to provide important ecosystem functions and services can be estimated with high confidence from GEDI, which illustrates its utility for applied ecological research. GEDI is thus an important step towards a global assessment of the structure and functioning of forest ecosystems.

Acknowledgments

References

Adam, M., Urbazaev, M., Dubois, C. & Schmullius, C. (2020) Accuracy assessment of GEDI terrain elevation and canopy height estimates in European temperate forests: influence of environmental and acquisition parameters. *Remote Sensing*, **12**, 3948.

Andrew, M.E., Wulder, M.A. & Nelson, T.A. (2014) Potential contributions of remote sensing to ecosystem service assessments. *Progress in Physical Geography: Earth and Environment*, **38**, 328–353.

Atkins, J.W., Bohrer, G., Fahey, R.T., Hardiman, B.S., Morin, T.H., Stovall, A.E.L. et al. (2018) Quantifying vegetation and canopy structural complexity from terrestrial LiDAR data using the forestr r package. *Methods in Ecology and Evolution*, **9**, 2057–2066.

AWN. (2018) *Waldentwicklungsplan 2018 + Südbünden*. Cantonal Office for Forest and Natural Hazards of Graubünden.

AWN. (2019) *Forest stand map*. Cantonal Office for Forest and Natural Hazards of Graubünden.

Baggio, T., Brožová, N., Bast, A., Bebi, P. & D'Agostino, V. (2022) Novel indices for snow avalanche protection assessment and monitoring of wind-disturbed forests. *Ecological Engineering*, **181**, 106677.

Banyard, T., Wright, C., Hindley, N., Halloran, G., Krisch, I., Kaifler, B. et al. (2021) Atmospheric gravity waves in Aeolus wind Lidar observations. *Geophysical Research Letters*, **48**, e2021GL092756.

Beck, J., Wirt, B., Armston, J., Hofton, M., Lutchke, S. & Tang, H. (2021) *GLOBAL Ecosystem Dynamics Investigation (GEDI) level 2 user guide.* For SDPS PGEVersion 3 (P003) of GEDI L2A Data and SDPS PGEVersion 3 (P003) of GEDI L2B Data. Available at: https://lpdaac.usgs.gov/documents/986/GEDI02_UserGuide_V2.pdf (Accessed 18 July 2022).

Becker, B. (2016) *Der Wald des Alpennationalparks Berchtesgaden – Zustand und Entwicklung – Dritte Waldinventur.*

Blaschke, T., Tiede, D. & Heurich, M. (2004) 3D landscape metrics to modelling forest structure and diversity based on laser scanning data. *International Archives of Photogrammetry, Remote Sensing and Spatial Information Sciences*, **XXXVI**, 129–132.

Bohn, F.J. & Huth, A. (2017) The importance of forest structure to biodiversity–productivity relationships. *Royal Society Open Science*, **4**, 160521.

Bouvier, M., Durrieu, S., Fournier, R. & Renaud, J.-P. (2015) Generalizing predictive models of forest inventory attributes using an area-based approach with airborne LiDAR data. *Remote Sensing of Environment*, **156**, 322–334.

Clawges, R., Vierling, K., Vierling, L. & Rowell, E. (2008) The use of airborne lidar to assess avian species diversity, density, and occurrence in a pine/aspen forest. *Remote Sensing of Environment*, **112**, 2064–2073.

Coops, N.C., Tompaski, P., Nijland, W., Rickbeil, G.J.M., Nielsen, S.E., Bater, C.W. et al. (2016) A forest structure habitat index based on airborne laser scanning data. *Ecological Indicators*, **67**, 346–357.

Depauw, L., Perring, M.P., Landuyt, D., Maes, S.L., Blondeel, H., Lombaerde, E. et al. (2021) Evaluating structural and compositional canopy characteristics to predict the light-demand signature of the forest understorey in mixed, semi-natural temperate forests. *Applied Vegetation Science*, **24**, e12532.

Dubayah, R., Blair, J.B., Goetz, S., Fatoyinbo, L., Hansen, M., Healey, S. et al. (2020) The global ecosystem dynamics investigation: high-resolution laser ranging of the Earth's forests and topography. *Science of Remote Sensing*, **1**, 100002.

Dubayah, R., Hofton, M., Blair, J., Armston, J., Tang, H. & Luthcke, S. (2021) *GEDI L2A elevation and height metrics data global footprint level V002*. NASA EOSDIS Land Processes DAAC. Available from: https://doi.org/10.5067/GEDI/GEDI02_A.002

Dubayah, R., Tang, H., Armston, J., Luthcke, S., Hofton, M. & Blair, J. (2021) *GEDI L2B canopy cover and vertical profile metrics data global footprint level V002*. NASA EOSDIS Land Processes DAAC. Available from: https://doi.org/10.5067/GEDI/GEDI02_B.002

Dubayah, S.L.R., Hofton, M., Blair, J.B., Armston, J., Tang, H. & Luthcke, S. (2020) *GEDI L2A elevation and height metrics data global footprint level V001*. NASA EOSDIS Land Processes DAAC.

Duncanson, L., Kellner, J.R., Armston, J., Dubayah, R., Minor, D.M., Hancock, S. et al. (2022) Aboveground biomass density models for NASA's global ecosystem dynamics investigation (GEDI) lidar mission. *Remote Sensing of Environment*, **270**, 112845.

Fang, H., Baret, F., Plummer, S. & Schaepman-Strub, G. (2019) An overview of global leaf area index (LAI): methods, products, validation, and applications. *Reviews of Geophysics*, **57**, 739–799.

FAO. (2020) *Global forest resources assessment 2020*. Available at: https://www.fao.org/documents/card/en/c/ca9825en (Accessed 18 July 2022).

Fayad, I., Baghdadi, N., Alcarde Alvares, C., Stape, J., Bailly, J.-S., Scolforo, H. et al. (2021) Terrain slope effect on forest height and wood volume estimation from GEDI data. *Remote Sensing*, **13**, 22.

Fayad, I., Baghdadi, N.N., Alvares, C.A., Stape, J.L., Bailly, J.S., Scolforo, H.F. et al. (2021) Assessment of GEDI's LiDAR data for the estimation of canopy heights and wood volume of eucalyptus plantations in Brazil. *IEEE Journal of Selected Topics in Applied Earth Observations and Remote Sensing*, **14**, 7095–7110.

Fayad, I., Ienco, D., Baghdadi, N., Gaetano, R., Alvares, C.A., Stape, J.L. et al. (2021) A CNN-based approach for the estimation of canopy heights and wood volume from GEDI waveforms. *Remote Sensing of Environment*, **265**, 112652.

Felipe-Lucia, M.R., Soliveres, S., Penone, C., Manning, P., van der Plas, F., Boch, S. et al. (2018) Multiple forest attributes underpin the supply of multiple ecosystem services. *Nature Communications*, **9**, 4839. Available from: https://doi.org/10.1038/s41467-018-07082-4

Frehner, M., Wasser, B. & Schwitter, R. (2005) *Nachhaltigkeit und Erfolgskontrolle im Schutzwald*. Schutzfunktion: Wegleitung für Pfl egemassnahmen in Wäldern mit.

Gao, Y., Skutsch, M., Paneque-Gálvez, J. & Ghilardi, A. (2020) Remote sensing of forest degradation: a review. *Environmental Research Letters*, **15**, 103301. Available from: https://doi.org/10.1088/1748-9326/abaad7

Garcia, M., Saatchi, S., Ferraz, A., Silva, C.A., Ustin, S., Koltunov, A. et al. (2017) Impact of data model and point

density on aboveground forest biomass estimation from airborne LiDAR. *Carbon Balance and Management*, **12**, 4. Available from: https://doi.org/10.1186/s13021-017-0073-1

Gelabert, P.J., Montealegre, A.L., Lamelas, M.T. & Domingo, D. (2020) Forest structural diversity characterization in Mediterranean landscapes affected by fires using airborne laser scanning data. *GIScience & Remote Sensing*, **57**, 497–509.

George, J.-P., Yang, W., Kobayashi, H., Biermann, T., Carrara, A., Cremonese, E. et al. (2021) Method comparison of indirect assessments of understory leaf area index (LAIu): a case study across the extended network of ICOS forest ecosystem sites in Europe. *Ecological Indicators*, **128**, 107841.

Graf, R., Mathys, L. & Bollmann, K. (2013) Habitat assessment for forest dwelling species using LiDAR remote sensing: Capercaillie in the Alps. *Forest Ecology and Management*, **257**, 160–167.

Grêt-Regamey, A. & Straub, D. (2006) Spatially explicit avalanche risk assessment linking Bayesian networks to a GIS. *Natural Hazards and Earth System Sciences*, **6**, 911–926.

Hancock, S., McGrath, C., Lowe, C., Davenport, I. & Woodhouse, I. (2019) Requirements for a global lidar system: spaceborne lidar with wall-to-wall coverage. *Royal Society Open Science*, **8**, 211166.

Heurich, M. & Thoma, F. (2008) Estimation of forestry stand parameters using laser scanning data in temperate, structurally rich natural European beech (*Fagus sylvatica*) and Norway spruce (*Picea abies*) forests. *Forestry: An International Journal of Forest Research*, **81**, 645–661.

Hiltner, U., Huth, A. & Fischer, R. (2022) Importance of the forest state in estimating biomass losses from tropical forests: combining dynamic forest models and remote sensing. *Biogeosciences*, **19**, 1911.

Hock, R., Rasul, G., Adler, C., Cáceres, B., Gruber, S., Hirabayashi, Y. et al. (2019) High mountain areas. In: Pörtner, H.-O., Roberts, D.C., Masson-Delmotte, V., Zhai, P., Tignor, M., Poloczanska, E. et al. (Eds.) *IPCC special report on the ocean and cryosphere in a changing climate* (pp. 131–202). Cambridge, UK and New York, NY: Cambridge University Press. Available from: https://doi.org/10.1017/9781009157964.004.

Hofton, M., Blair, J.B., Story, S. & Yi, D. (2019) *Algorithm Theoretical Basis Document (ATBD) for GEDI transmit and receive waveform processing for L1 and L2 products*.

Jarron, L.R., Coops, N.C., MacKenzie, W.H., Tompalski, P. & Dykstra, P. (2020) Detection of sub-canopy forest structure using airborne LiDAR. *Remote Sensing of Environment*, **244**, 111770.

Jucker, T. (2022) Deciphering the fingerprint of disturbance on the three-dimensional structure of the world's forests. *New Phytologist*, **233**, 612–617.

Kortmann, M., Heurich, M., Latifi, H., Rösner, S., Seidl, R., Müller, J. et al. (2018) Forest structure following natural disturbances and early succession provides habitat for two avian flagship species, capercaillie (*Tetrao urogallus*) and hazel grouse (*Tetrastes bonasia*). *Biological Conservation*, **226**, 81–91.

Kucharik, C.J., Norman, J.M. & Gower, S.T. (1998) Measurements of branch area and adjusting leaf area index indirect measurements. *Agricultural and Forest Meteorology*, **91**, 69–88.

Kutchartt, E., Pedron, M. & Pirotti, F. (2022) Assessment of canopy and ground height accuracy from GEDI LIDAR OVER steep mountain areas. *ISPRS Annals of the Photogrammetry, Remote Sensing and Spatial Information Sciences*, **V-3-2022**, 431–438.

Lang, N., Kalischek, N., Armston, J., Schindler, K., Dubayah, R. & Wegner, J.D. (2022) Global canopy height regression and uncertainty estimation from GEDI LIDAR waveforms with deep ensembles. *Remote Sensing of Environment*, **268**, 112760.

LaRue, E.A., Fahey, R., Fuson, T.L., Foster, J.R., Matthes, J.H., Krause, K. et al. (2022) Evaluating the sensitivity of forest structural diversity characterization to LiDAR point density. *Ecosphere*, **13**, e4209.

Lefsky, M.A., Cohen, W.B., Parker, G.G. & Harding, D.J. (2002) Lidar remote sensing for ecosystem studies: Lidar, an emerging remote sensing technology that directly measures the three-dimensional distribution of plant canopies, can accurately estimate vegetation structural attributes and should be of particular interest to forest, landscape, and global ecologists. *Bioscience*, **52**, 19–30.

Li, Z., Strahler, A., Schaaf, C., Jupp, D., Schaefer, M. & Olofsson, P. (2018) Seasonal change of leaf and woody area profiles in a midlatitude deciduous forest canopy from classified dual-wavelength terrestrial lidar point clouds. *Agricultural and Forest Meteorology*, **262**, 279–297.

Lim, K., Treitz, P., Wulder, M., St-Onge, B. & Flood, M. (2003) LiDAR remote sensing of forest structure. *Progress in Physical Geography: Earth and Environment*, **27**, 88–106.

Liu, A., Cheng, X. & Chen, Z. (2021) Performance evaluation of GEDI and ICESat-2 laser altimeter data for terrain and canopy height retrievals. *Remote Sensing of Environment*, **264**, 112571.

Lotz, A. (2006) *Alpine habitat diversity–HABITALP–project report 2002–2006*. EU Community Initiative INTERREG III B Alpine Space Programme. Nationalpark Berchtesgaden.

Luthcke, S., Rebold, T., Thomas, T. & Pennington, T. (2019) *Algorithm Theoretical Basis Document (ATBD) for GEDI waveform geolocation for L1 and L2 products*. NASA Goddard Space Flight Center, Emergent Space Technologies, KBR Greenbelt. Available at: https://lpdaac.usgs.gov/documents/579/GEDI__WFGEO_ATBD_v1.0.pdf (Accessed 18 July 2022).

MacArthur, R.H. & MacArthur, J.W. (1961) On bird species diversity. *Ecology*, **42**, 594–598.

Mayer, H. (1984) *Wälder Europas*. München: G. Fischer Verlag.

McDowell, N.G., Allen, C.D., Anderson-Teixeira, K., Aukema, B.H., Bond-Lamberty, B., Chini, L. et al. (2020) Pervasive shifts in forest dynamics in a changing world. *Science*, **368**, eaaz9463.

Melin, M., Hinsley, S.A., Broughton, R.K., Bellamy, P. & Hill, R.A. (2018) Living on the edge: utilising lidar data to assess the importance of vegetation structure for avian diversity in fragmented woodlands and their edges. *Landscape Ecology*, **33**, 895–910. Available from: https://doi.org/10.1007/s10980-018-0639-7

Mietkiewicz, N., Kulakowski, D., Rogan, J. & Bebi, P. (2017) Long-term change in sub-alpine forest cover, tree line and species composition in the Swiss Alps. *Journal of Vegetation Science*, **28**, 951–964.

Moeslund, J.E., Zlinszky, A., Ejrnæs, R., Brunbjerg, A.K., Bøcher, P.K., Svenning, J.-C. et al. (2019) Light detection and ranging explains diversity of plants, fungi, lichens, and bryophytes across multiple habitats and large geographic extent. *Ecological Applications*, **29**, e01907.

Næsset, E. (1997) Determination of mean tree height of forest stands using airborne laser scanner data. *ISPRS Journal of Photogrammetry and Remote Sensing*, **52**, 49–56.

Ni, W., Zhang, Z. & Sun, G. (2021) Assessment of slope-adaptive metrics of GEDI waveforms for estimations of Forest aboveground biomass over mountainous areas. *Journal of Remote Sensing*, **2021**, 9805364. Available from: https://doi.org/10.34133/2021/9805364

Potapov, P., Li, X., Hernandez-Serna, A., Tyukavina, A., Hansen, M.C., Kommareddy, A. et al. (2021) Mapping global forest canopy height through integration of GEDI and Landsat data. *Remote Sensing of Environment*, **253**, 112165.

R Core Team. (2021) *R: a language and environment for statistical computing*. Vienna, Austria: R Foundation for Statistical Computing.

Roussel, J. & Auty, D. (2022) *Airborne LiDAR data manipulation and visualization for forestry applications*. R package version 4.0.1. Available at: https://cran.r-project.org/package=lidR (Accessed 18 July 2022).

Roussel, J.R., Auty, D., Coops, N.C., Tompalski, P., Goodbody, T.R.H., Sánchez Meador, A. et al. (2020) lidR: an R package for analysis of airborne laser scanning (ALS) data. *Remote Sensing of Environment.*, **251**, 112061.

Roussel, J.-R., Béland, M., Caspersen, J. & Achim, A. (2018) A mathematical framework to describe the effect of beam incidence angle on metrics derived from airborne LiDAR: the case of forest canopies approaching turbid medium behaviour. *Remote Sensing of Environment*, **209**, 824–834.

Roy, D.P., Kashongwe, H.B. & Armston, J. (2021) The impact of geolocation uncertainty on GEDI tropical forest canopy height estimation and change monitoring. *Science of Remote Sensing*, **4**, 100024.

Schneider, F.D., Ferraz, A., Hancock, S., Duncanson, L., Dubayah, R., Pavlick, R. et al. (2020) Towards mapping the diversity of canopy structure from space with GEDI. *Environmental Research Letters*, **15**, 115006.

Schutz, B., Zwally, H., Shuman, C.A. & Hancock, D. (2005) Overview of the ICESat mission. *Geophysical Research Letters*, **32**, L21S01.

Sebald, J., Senf, C., Heiser, M., Scheidl, C., Pflugmacher, D. & Seidl, R. (2019) The effects of forest cover and disturbance on torrential hazards: large-scale evidence from the eastern Alps. *Environmental Research Letters*, **14**, 114032. Available from: https://doi.org/10.1088/1748-9326/ab4937

Seidl, R., Spies, T.A., Rammer, W., Steel, E.A., Pabst, R.J. & Olsen, K. (2012) Multi-scale drivers of spatial variation in old-growth Forest carbon density disentangled with Lidar and an individual-based landscape model. *Ecosystems*, **15**, 1321–1335. Available from: https://doi.org/10.1007/s10021-012-9587-2

Senf, C. & Seidl, R. (2022) Post-disturbance canopy recovery and the resilience of Europe's forests. *Global Ecology and Biogeography*, **31**, 25–36. Available from: https://doi.org/10.1111/geb.13406

Shannon, C.E. (1948) A mathematical theory of communication. *Bell System Technical Journal*, **27**, 379–423.

Silva, C., Hamamura, C., Valbuena, R., Hancock, S., Cardil, A., Broadbent, E. et al. (2020) rGEDI: an R package for NASA's global ecosystem dynamics investigation (GEDI) data visualizing and processing.

Stritih, A., Bebi, P., Rossi, C. & Grêt-Regamey, A. (2021) Addressing disturbance risk to mountain forest ecosystem services. *Journal of Environmental Management*, **296**, 113188.

Suter, W., Graf, R.F. & Hess, R. (2002) Capercaillie (*Tetrao urogallus*) and avian biodiversity: testing the umbrella-species concept. *Conservation Biology*, **16**, 778–788.

Tang, H. & Armston, J. (2019) *Algorithm theoretical basis document (ATBD) for GEDI L2B footprint canopy cover and vertical profile metrics*. Greenbelt, MD, USA: Goddard Space Flight Center.

Tang, H., Armston, J., Hancock, S., Marselis, S., Goetz, S. & Dubayah, R. (2019) Characterizing global forest canopy cover distribution using spaceborne lidar. *Remote Sensing of Environment*, **231**, 111262.

Taskinen, S. & Warton, D. (2011) Robust estimation and inference for bivariate line-fitting in allometry. *Biometrische Zeitschrift*, **53**, 652–672.

Temperli, C., Stadelmann, G., Thürig, E. & Brang, P. (2017) Silvicultural strategies for increased timber harvesting in a central European mountain landscape. *European Journal of Forest Research*, **136**, 1–17.

Thom, D., Rammer, W., Laux, P., Smiatek, G., Kunstmann, H., Seibold, S. et al. (2022) Will forest dynamics continue to accelerate throughout the 21st century in the northern Alps? *Global Change Biology*, **28**, 3260–3274.

Thom, D. & Seidl, R. (2022) accelerating mountain forest dynamics in the Alps. *Ecosystems*, **25**, 603–617. Available from: https://doi.org/10.1007/s10021-021-00674-0

Valbuena, R., O'Connor, B., Zellweger, F., Simonson, W., Vihervaara, P., Maltamo, M. et al. (2020) Standardizing ecosystem morphological traits from 3D information sources. *Trends in Ecology & Evolution*, **35**, 656–667.

Vauhkonen, J. (2018) Predicting the provisioning potential of forest ecosystem services using airborne laser scanning data and forest resource maps. *Forest Ecosystems*, **5**, 1–19. Available from: https://doi.org/10.1186/s40663-018-0143-1

Viana-Soto, A., García, M., Aguado, I. & Salas, J. (2022) Assessing post-fire forest structure recovery by combining LiDAR data and Landsat time series in Mediterranean pine forests. *International Journal of Applied Earth Observation and Geoinformation*, **108**, 102754.

Walter, J.A., Stovall, A.E.L. & Atkins, J.W. (2021) Vegetation structural complexity and biodiversity in the Great Smoky Mountains. *Ecosphere*, **12**, e03390.

Wang, Y., Ni, W., Sun, G., Chi, H., Zhang, Z. & Guo, Z. (2019) Slope-adaptive waveform metrics of large footprint lidar for estimation of forest aboveground biomass. *Remote Sensing of Environment*, **224**, 386–400.

Warton, D.I., Duursma, R.A., Falster, D.S. & Taskinen, S. (2012) Smatr 3 – an R package for estimation and inference about allometric lines. *Methods in Ecology and Evolution*, **3**, 257–259.

Warton, D.I. & Weber, N.C. (2002) Common slope tests for bivariate errors-in-variables models. *Biometrical Journal*, **44**, 161–174.

Warton, D.I., Wright, I.J., Falster, D.S. & Westoby, M. (2006) Bivariate line-fitting methods for allometry. *Biological Reviews of the Cambridge Philosophical Society*, **81**, 259–291.

Watt, A.S. (1947) Pattern and process in the plant community. *Journal of Ecology*, **35**, 1–22.

Whittaker, R.H. & Woodwell, G.M. (1969) Structure, production and diversity of the oak-pine Forest at Brookhaven, New York. *Journal of Ecology*, **57**, 155.

Winker, D.M. (2007) The CALIPSO Mission and initial observations of aerosols and clouds from CALIOP. In: *Fourier transform spectroscopy/hyperspectral imaging and sounding of the environment (HTuD1)*. Santa Fe, New Mexico: Optica Publishing Group.

Winkler, K., Fuchs, R., Rounsevell, M. & Herold, M. (2021) Global land use changes are four times greater than previously estimated. *Nature Communications*, **12**, 2501. Available from: https://doi.org/10.1038/s41467-021-22702-2

Wulder, M.A., Hermosilla, T., Stinson, G., Gougeon, F.A., White, J.C., Hill, D.A. et al. (2020) Satellite-based time series land cover and change information to map forest area consistent with national and international reporting requirements. *Forestry: An International Journal of Forest Research*, **93**, 331–343.

Zhao, W., Tan, W. & Li, S. (2021) High leaf area index inhibits net primary production in global temperate forest ecosystems. *Environmental Science and Pollution Research*, **28**, 22602–22611. Available from: https://doi.org/10.1007/s11356-020-11928-0

Zolkos, S., Goetz, S. & Dubayah, R. (2013) A meta-analysis of terrestrial aboveground biomass estimation using lidar remote sensing. *Remote Sensing of Environment*, **128**, 289–298.